

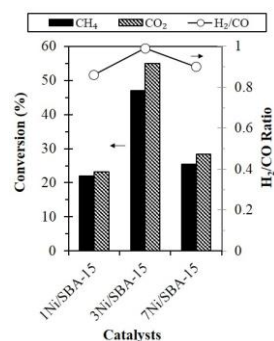
Production of syngas via CO₂ reforming of methane over Ni/SBA-15Nurul Ainirazali^{a*}, Herma Dina Setiabudi^a, Dai-Viet N. Vo^{a,b}, Siti Nuraihan Mohamad Arof^a^aFaculty of Chemical and Natural Resources Engineering, Universiti Malaysia Pahang, Lebuhraya Tun Razak, 26300 Gambang, Kuantan, Pahang, Malaysia^bCentre of Excellence for Advanced Research in Fluid Flow, Universiti Malaysia Pahang, 26300 Gambang, Kuantan, Pahang, Malaysia

*Corresponding author email: ainirazali@ump.edu.my (Nurul Ainirazali)

Article history :

Received 23 November 2016

Accepted 10 April 2017

GRAPHICAL ABSTRACT**ABSTRACT**

In the present study, the effect of Ni loading (1-7 wt.%) on the properties of Ni/SBA-15 and CO₂ reforming of methane were studied. Ni/SBA-15 catalyst was synthesized by sol-gel method and was characterized by XRD, BET, TEM and FTIR to study the physicochemical properties. The catalyst was evaluated for CO₂ reforming of methane at 800 °C using fixed bed reactor. The N₂ adsorption-desorption results confirmed that all the samples present the ordered mesoporous structure of SBA-15, where the surface area, pore volume and pore diameter were decreased as the Ni loading increased. Moreover, the dispersion of Ni species and formation of NiO crystallite size are depending on the wt.% of Ni loading on SBA-15 support which directly related to the substitution of surface silanol group with Ni species. Catalytic activity test revealed that the optimum Ni loading was at 3 wt.% with the CH₄ conversion, CO₂ conversion and H₂/CO ratio was about 55%, 47%, and 0.99, respectively. Meanwhile, higher Ni loading (7 wt.%) decreased the catalytic performance of catalyst due to the agglomeration of Ni particles on the SBA-15 surfaces which led to easier sintering and carbon deposition on the catalyst surfaces.

Keywords: Dry reforming; Carbon monoxide; Hydrogen; Ni dispersion; Mesoporous

© 2017 Dept. of Chemistry, UTM. All rights reserved
| eISSN 0128-2581 |

1. INTRODUCTION

The study of methane reforming with CO₂, also known as dry reforming has gained a significant interest in view of environmental perspective for conversion of undesirable greenhouse gases to added value product. A lot of studies on the CO₂ reforming of methane have shown that Ni-based catalyst was the most efficient catalyst for the production of H₂ and syngas comparable in some studies to the noble metals [1-3]. The performance of the Ni-based catalysts are influenced by many factors such as the type of support materials, Ni loading, Ni dispersion, and preparation method of catalyst. Moreover, the most important challenges for CO₂ reforming reaction is coke deposition over the surface of catalyst due to the sintering of both active metals and support during the reaction. This phenomenon results in physical blocking of active sites on the catalyst surfaces which further reduce the catalytic activity [4,5].

Up to now, various supported metal catalysts have been successfully applied for CO₂ reforming of methane, especially noble (Pt, Re, Pd, Ir) and transition (Ni, Fe, Mg) metals. Among the catalyst, the noble metals based catalyst was reported to be a good carbon deposition resistance and more active towards the CO₂ reforming [2-4]. Transition metal based catalysts are more promising to be used for commercialization due to its easy availability, high activity and cheap [5-7]. However, deactivation arising from carbon

deposition which favorable by the transition metals would limits the reaction and lifespan of the catalyst. One way to suppress the formation of carbon deposition is by using a good support with appropriate properties. Nowadays, researchers struggled to develop a more stable and good properties of support material to improve the catalytic behavior. It is well known that the support's nature would affect the physical and chemical properties of the catalyst, especially in the dispersion of active sites on the catalyst surfaces, which then determine the activity and selectivity of the catalysts.

Mesoporous SBA-15 silica acts represent a potential support material due to its uniform hexagonal channels (3 to 30 nm), high surface area (600-1000 m²/g), excellent thermal stability, uniform pore diameter (5-30 nm), and thick pore wall [8, 9]. However, purely mesoporous SBA-15 silica alone could not act as active site in most catalytic applications [8]. Therefore, numerous efforts have been made in introducing catalytically active sites such as metals and metal oxides into the mesoporous SBA-15 silica [8-10]. It is well understood that the Ni loading on the support affects the Ni dispersion on the support surfaces and the Ni active sites interaction with the support, which further contribute to the catalytic behavior of the catalyst [1, 4]. Therefore, recently, we focus our attention on the effects of Ni dispersion and interaction with the SBA-15 for the reforming of methane with CO₂.

2. EXPERIMENTS

2.1 Catalyst synthesis

Ni/SBA-15 catalysts with different Ni loading (1, 3 and 7 wt.%) were synthesized by sol-gel method. Specifically, triblock Pluronic P123 copolymer ($M_{av}=5800$, EO₂₀PO₇₀E₂₀, Aldrich) was used as the structure-directing agent and tetraethyl orthosilicate (TEOS, Aldrich, 99.99%) as the silica source. 6.0 g P123 was dissolved in 12.5 g TEOS under vigorous stirring at 60 °C for about 15 min to obtain a homogeneous solution. Then, 25.0 g ethanol solution containing a requisite amount of Ni salt precursor, Ni(NO₃)₃·6H₂O (Merck, 99%) was added to the solution and stirred at 60 °C. 0.05 mol/L. HCl was added and the mixture was then stirred for 24 h until the green gel was formed. The sample was dried in an oven at 110 °C for 12 h and then calcined in air at 550 °C for 6 h.

2.2 Catalyst characterization

The characteristics of the synthesized catalysts were investigated using XRD, BET, TEM and FTIR. The crystalline structure of the catalyst was determined with X-ray diffraction (XRD) recorded on powder diffractometer (Rigaku model MiniflexII, 30 kW) using a Cu K α radiation ($\lambda = 1.5405\text{\AA}$) in the range of $2\theta = 10 - 80^\circ$. The measurement of multi-point BET surface area, pore diameter and pore volume for catalysts were conducted using AUTOSORB-1 model AS1 MP-LP instrument at 77 K. The structural morphologies of the catalysts were analyzed using a Philip CM12 transmission electron microscope (TEM) operated at 80 kV. Fourier-transform Infrared (FTIR) Spectroscopy analysis was carried out using Thermo Nicolet Avatar 370 DTGS model in KBr matrix in the range of 500 – 4000 cm⁻¹ in order to study the chemical properties of catalyst and to identify the interaction of Ni species with SBA-15.

2.3 Catalyst activity test

The CO₂ reforming of methane was conducted in a fixed bed reactor at 800 °C and atmospheric pressure. 0.2 g of catalysts was packed and placed vertically in a tubular furnace. Prior to the reaction, the catalyst was reduced in a H₂ flow of 50 ml/min for 3 h at 700 °C. Then, a mixture of CH₄ and CO₂ was fed into the reactor at CH₄/CO₂ ratio of 1. The composition of gaseous effluent from the reactor outlet was analyzed with an Agilent 6890 Series gas chromatograph (GC) equipped with thermal conductivity (TCD) detectors. The CO₂ and methane conversion (X) were calculated according to the following equations (1) and (2). Additionally, the product distribution ratio, H₂/CO was calculated based on equation (3);

$$X_{CO_2} = \frac{A_{CO_2,in} - A_{CO_2,out}}{A_{CO_2,in}} \times 100\% \quad (1)$$

$$X_{CH_4} = \frac{A_{CH_4,in} - A_{CH_4,out}}{A_{CH_4,in}} \times 100\% \quad (2)$$

$$\frac{H_2}{CO} = \frac{A_{H_2}}{A_{CO}} \quad (3)$$

where A is the corrected chromatographic area for particular compound.

3. RESULTS AND DISCUSSION

3.1 Characterization of catalysts

The X-ray diffraction (XRD) patterns of Ni/SBA-15 catalysts with different Ni loading were given in Fig. 1. The characteristic of the amorphous SiO₂ wall of SBA-15 was indicated by a broad diffraction peak centered at $2\theta \approx 23.5^\circ$ [4, 11]. This indicated that the ordered structure of mesoporous SBA-15 was remained by introduction of Ni up to 7 wt%. However, the intensities of the SBA-15 reflections were decreased with the increasing of Ni loading due to the disturbance of ordered mesostructure by Ni after catalyst preparation. The presence of sharp diffraction peaks at 37.3°, 43.3°, 44.5°, 51.8°, 63.0°, and 76.4° attributed to face-centered cubic crystalline NiO [4, 12]. The peaks were more intense with the increasing of Ni loading. This suggested that the much higher crystallite phase of NiO was located on the outer surface of SBA-15 from 1 to 7 wt.% of Ni loading. The estimated average crystallite size of 1Ni/SBA-15, 3Ni/SBA-15 and 7Ni/SBA-15 which was calculated using Scherrer equation were 7.5, 8.7 and 12.4 nm, respectively. This result pointed out that the Ni oxide dispersion decreased with an increase in the Ni loading from 1 to 7 wt.% which led to the agglomeration of Ni oxide species.

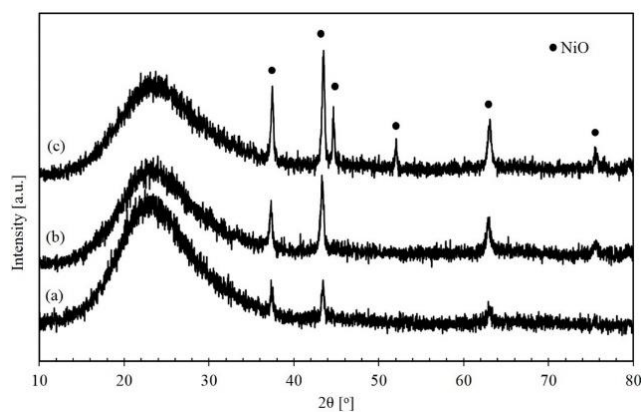


Fig. 1 XRD patterns of (a) 1Ni/SBA-15; (b) 3Ni/SBA-15 and (c) 7Ni/SBA-15.

Nitrogen adsorption/desorption isotherm of Ni/SBA-15 catalysts are shown in Fig. 2. All the sorption isotherms curves were classified as typical type IV with a H1 hysteresis loop, revealed the characteristic of ordered mesoporous materials of SBA-15 [13, 14]. The physical properties of Ni/SBA-15 catalysts are presented in Table 1. The BET surface area of 1Ni/SBA-15, 3Ni/SBA-15 and 7Ni/SBA-15 were 776.36, 651.91 and 622.84 m^2g^{-1} , respectively. Further decrease in BET surface area was noticed as Ni loading was increased, suggesting that the partial blockage of SBA-15 pores by the Ni metal particles [14]. The change in the BET surface area of the catalyst which caused by the different amounts of Ni loading was observed for Ni/MSN catalyst, reported by Aziz et al. [12]. They observed that the increasing in amount of Ni loading (1 – 10 wt.%) led to a decrease in the surface area of the MSN catalysts due to the blockage of the pores with Ni particles. The average pore volume and pore diameter were almost the same indicating that most of Ni metal particles were preferentially dispersed outside the SBA-15 pores. A similar phenomenon for 10Ni/SBA-15 caused by different preparation method was reported by Lu and Kawamoto [15].

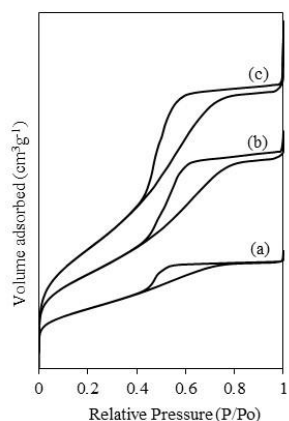


Fig. 2. Nitrogen adsorption/desorption isotherms of (a) 7Ni/SBA-15 and (b) 3Ni/SBA-15 and (c) 1Ni/SBA-15 catalysts.

Table 1. Textural properties of 1Ni/SBA-15, 3Ni/SBA-15 and 7Ni/SBA-15 catalysts.

Catalyst	BET surface area (m^2g^{-1})	Total pore volume (cm^3g^{-1})	Average pore diameter (nm)	Ni crystallite size ^a (nm)
1Ni/SBA-15	776.36	0.72	3.86	7.5
3Ni/SBA-15	651.91	0.66	3.82	8.7
7Ni/SBA-15	622.84	0.61	3.70	12.4

^a Estimated using the Scherrer equation

Further dispersions of the reduced Ni species on the SBA-15 support was confirmed by TEM analysis. Fig. 3(A) shows the TEM images of the 3Ni/SBA-15, considerable number of metallic Ni nanoparticles with the size around 8-10 nm were dispersed on the external surface of the SBA-15. While, larger Ni nanoparticles with average particles size between 10-15 nm were observed for 7Ni/SBA-15 (Fig. 3(B)), probably due to the aggregation during calcination

process, leading to lower dispersion of Ni species on the SBA-15 surface. This result is in line with the XRD results, where higher intensities of the metallic Ni crystallite was detected due to the larger size of the Ni species.

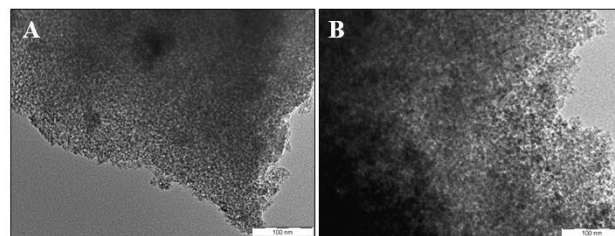


Fig. 3. TEM image of (A) 3Ni/SBA-15 and (B) 7Ni/SBA-15

The FTIR spectra of Ni/SBA-15 catalysts in the range of 1400 – 500 cm^{-1} and 3700 – 2500 cm^{-1} were shown in Fig. 4. The band at 3420 cm^{-1} was attributed to the stretching vibrations of the surface silanol groups and the adsorbed H_2O [16]. The band at approximately 801 cm^{-1} and 1040 cm^{-1} was attributed to the symmetric stretching vibration (Si-O-Si)_{sym} of tetrahedral SiO_4 structure and the anti-symmetric vibration nonbridging oxygen atoms (Si-O^δ) of Si-O-H bonds, respectively [17]. These Si-O-Si bands at 801 cm^{-1} and 1040 cm^{-1} were associated with the condensed silica network formation of SBA-15 was reported by Ma et al [18]. In addition, the band at approximately 520 cm^{-1} was related to the tetrahedral bending of Si-O bonds [19]. It was observed that the band at 3420 cm^{-1} was slightly decreased as the Ni content increased evidenced by the formation of Si-O-Ni after substitution of O-H with O-Ni. The peak at 3420 cm^{-1} was related to the intensity of O-H stretching vibration mode of Si-OH involved in hydrogen interaction with the adsorbed water molecule of the catalyst. Moreover, the presence of band at around 961 cm^{-1} was generally attributed to the bonding of SiO units to the metal, evidenced in the interaction of Ni with Si-O^δ of SBA-15 by the substitution of O-H with O-Ni [19-21]. However, the intensities of the band at 801 cm^{-1} and 520 cm^{-1} were remained due to the (Si-O-Si)_{sym} and tetrahedral bending of Si-O bonds interacted with Ni.

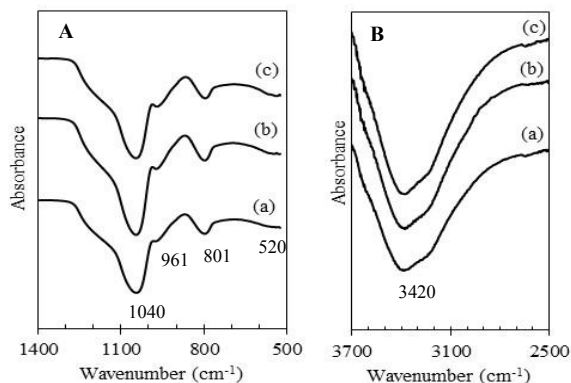


Fig. 4. FTIR spectra of (a) 1Ni/SBA-15; (b) 3Ni/SBA-15 and (c) 7Ni/SBA-15 catalysts in the range of (A) 1400 – 500 cm^{-1} ; (B) 3700 – 2500 cm^{-1} .

Studies on the structural changes of SBA-15 altered by Ti metal addition was done by Ye et al. [19]. They observed that the new band at 966 cm^{-1} appeared probably due to the silica tetrahedron framework which incorporated with Ti metal.

3.2 CO₂ reforming of methane

To understand the nature influence of active sites on the catalytic activity of CO₂ reforming of methane, different Ni loading on SBA-15 was investigated. The results of Ni/SBA-15 catalytic performance for CH₄ conversion, CO₂ conversion and H₂/CO ratio are shown in Fig. 5. The results revealed that the presence of Ni species could increase the catalytic reaction. As can be seen in all samples, conversion of CO₂ was higher than CH₄ conversion and the H₂/CO ratio was less than one because of the influence from reverse water-gas shift reaction. These fact phenomena were in good agreements with those reported for CO₂ reforming of methane [1, 4]. The catalysts activities for CO₂ reforming of methane were most active in the following order: 3Ni/SBA-15 > 7Ni/SBA-15 > 1Ni/SBA-15. It was observed that the 3Ni/SBA-15 catalyst showed the highest CO₂ conversion

(55%), CH₄ conversion (47%) and H₂/CO ratio (0.99), suggesting that this modified catalyst could provide sufficient Ni active sites for the reactants to be converted to syngas under the experimental conditions tested. Moreover, the best catalytic behavior of 3Ni/SBA-15 was probably related to the substitution of sufficient Ni species with the surface silanol groups as evidenced by FTIR analysis. In addition, good dispersion of Ni species is also a key factor influencing the catalyst activity. 3Ni/SBA-15 had the higher activities probably due to the good dispersion of optimal Ni loading, while poor catalytic performance of 7Ni/SBA-15 might due to the agglomeration of Ni particles on the SBA-15 surface. Combining the XRD (Fig. 1), N₂ physisorption (Table. 1) and FTIR analysis (Fig. 4) results, 7Ni/SBA-15 exhibited higher surface of Ni content than other catalysts. Yang et al [4] reported that higher surface Ni content would lead to easier sintering and carbon deposition on the catalyst surfaces. This phenomenon led to the poor catalyst activity and stability as evidenced by 7Ni/SBA-15 catalyst. Meanwhile, the poor performance of 1Ni/SBA-15 suggested the less active sites of Ni species on the SBA-15 surface.

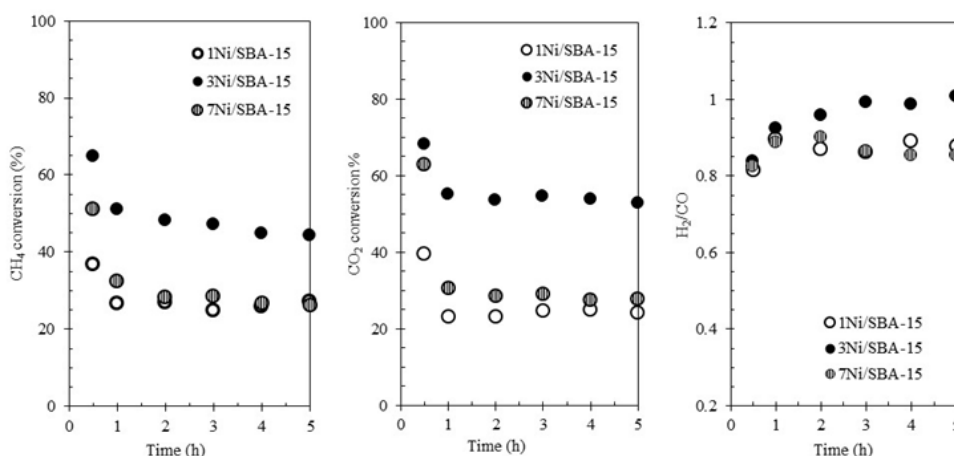


Fig. 5 Effect of different Ni loading on (a) CH₄ conversion; (b) CO₂ conversion and (c) H₂/CO ratio.

4. CONCLUSION

The promotional effect of Ni loading on the SBA-15 support towards the physicochemical and catalytic CO₂ reforming of methane were investigated. XRD, BET and FTIR results summarized that the increasing Ni loading from 1 to 7 wt% decreased the crystallinity, surface area, pore volume, pore diameter and physically absorbed water content of the catalysts. These results were suggested due to the substitution of surface silanol groups of SBA-15 support with Ni species. Among the catalysts, 3 wt.% of Ni loading on the SBA-15 (3Ni/SBA-15) support prepared via sol-gel method had optimum Ni active sites, performed higher

activity with CO₂ conversion, CH₄ conversion, and H₂/CO ratio of 55%, 47%, and 0.99, respectively. However, higher Ni loading (7Ni/SBA-15) decreased the catalytic performance of catalyst due to the agglomeration of Ni particles which lead to easier sintering and carbon deposition on the catalyst surfaces.

ACKNOWLEDGEMENTS

The authors are grateful for the financial support RDU170330, RDU140391 and RDU140398 granted by Universiti Malaysia Pahang and RDU150126 granted by Ministry of Higher Education, Malaysia.

REFERENCES

- [1] Z. Alipour, M. Rezaei, F. Meshkani, *Fuel* 129 (2014) 197.
- [2] E.C. Faria, R.C.R. Neto, R.C. Colman, F.B. Noronha, *Catal. Today* 228 (2014) 138.
- [3] F. Rahmani, M. Haghighi, Y. Vafaeian, P. Estifae, *J. Power Sources* 272 (2014) 816.
- [4] W. Yang, H. Liu, Y. Li, H. Wu, D. He, *Int. J. Hydrogen Energy* 41 (2015) 1513-1523.
- [5] A. Vita, G. Cristiano, C. Italiano, L. Pino, S. Specchia, *Appl. Catal. B* 162 (2015) 551.
- [6] F. Wang, L. Xu, W. Shi, J. CO₂ Util. *J. CO₂ Util.* 16 (2016) 318.
- [7] H.D. Setiabudi, K.H. Lim, N. Ainirazali, S.Y. Chin, N.H.N. Kamarudin, *J. Mater. Environ. Sci.* 8 (2017) 573
- [8] Q. Tang, S. Hu, Y. Chen, Z. Guo, Y. Hu, Y. Chen, Y. Yang, *Microporous Mesoporous Mater.* 132 (2010) 501-509.
- [9] M. Tao, X. Meng, Y. Lv, Z. Bian, Z. Xin, *Fuel* 165 (2016) 289.
- [10] A.K. Medina-Mendoza, M.A. Cortés-Jácome, J.A. Toledo-Antonio, C. Angeles-Chávez, E. López-Salinas, I. Cuauhtémoc-López, M.C. Barrera, J. Escobar, J. Navarrete, I. Hernández, *Appl. Catal. B* 106 (2011) 14.
- [11] Ł. Laskowski, M. Laskowska, M. Bałanda, M. Fitta, J. Kwiatkowska, K. Dziliński, A. Karczmarzka, *Microporous Mesoporous Mater.* 200 (2014) 253.
- [12] M.A.A. Aziz, A.A. Jalil, S. Triwahyono, M.W.A. Saad, *Chem. Eng. J.* 260 (2015) 757.
- [13] N. Anand, P. Ramudu, K.H.P. Reddy, K.S.R. Rao, B. Jagadeesh, V.S.P. Babu, D.R. Burri, *Appl. Catal. A* 454 (2013) 119.
- [14] R. Ghorbani-Vaghei, S. Hemmati, H. Veisi, *J. Mol. Catal. A* 393 (2014) 240.
- [15] B. Lu, K. Kawamoto, *Fuel* 103 (2013) 699.
- [16] E.G. Mahoney, J.M. Pusel, S.M. Stagg-Williams, S. Faraji, *J. CO₂ Util.* 6 (2014) 40.
- [17] X.-Y. Quek, D. Liu, W.N.E. Cheo, H. Wang, Y. Chen, Y. Yang, *Appl. Catal. B* 95 (2010) 374.
- [18] Z. Ma, X. Wang, S. Wei, H. Yang, F. Zhang, P. Wang, M. Xie, *J. Ma, Catal. Com.* 39 (2013) 24.
- [19] W. Ye, Z. Lin, B. Dong, J. Kang, X. Zheng, X. Wang, *Mater. Sci. App.* 2 (2011) 661.
- [20] Y.T. Fang, T. Liu, Z. C. Zhang, X. N. Gao, *Renew. Energy* 63 (2014) 755.
- [21] V. Subbaramaiah, V. C. Srivastava, I.D. Mall, *J. of Hazard. Mater.* 248-249 (2013) 355.